Available online at www.sciencedirect.com
SCIENCE DIRECT®
Bioorganic & Medicinal Chemistry 14 (2006) 641–649
Bioorganic & Medicinal Chemistry

# Polymeric grape-seed procyanidins, but not monomeric catechins and oligomeric procyanidins, impair degranulation and membrane ruffling in RBL-2H3 cells

Kazunari Kondo,[a,*] Riichiro Uchida,[b] Shoichi Tokutake[b] and Tamio Maitani[a]

[a]*Division of Foods, National Institute of Health Sciences, Kamiyoga 1-18-1, Setagaya, Tokyo 158-8501, Japan*
[b]*Research and Development Division, Kikkoman Corporation, 399 Noda, Noda City, Chiba 278-0037, Japan*

Received 12 July 2005; revised 23 August 2005; accepted 23 August 2005
Available online 27 September 2005

**Abstract**—Grape-seed proanthocyanidins (GSPs) are catechin polymers that are predicted to form helices in their global minimum-energy conformation and to have a mean degree of polymerization of seven (mDP = 7). The highly polymerized GSP-H fraction (mDP = 10) was found to impair degranulation in RBL-2H3 cells after stimulation with an antigen (Ag) and treatment with the Ca-ATPase inhibitor thapsigargin (Tg). In addition, GSP-H affected actin cytoskeleton and inhibited membrane ruffling in these cells, resulting in the suppression of exocytosis. By contrast, monomeric epicatechin, the dimeric procyanidins PA-1, PA-2, and PB-2, and the oligomerized GSP-L (mDP = 3) had no effect on membrane ruffling and degranulation. These findings indicate that the molecular size and length of GSP-H are needed for the inhibition of membrane ruffling and degranulation in RBL-2H3 mast-cell lines.


## 1. Introduction

Proanthocyanidins are a mixture of monomers, oligomers, and polymers of flavan-3-ols (known as catechins), which are ubiquitous in plants. Proanthocyanidins act as antioxidants scavenging free radicals[1–3] and are thought to prevent ischemia/reperfusion damage caused by reactive oxygen species such as superoxides and peroxynitrites.[4] Green tea antioxidants have recently been shown to block neutrophil-mediated angiogenesis in vivo and to inhibit chemokine-induced neutrophil chemotaxis in vitro. Dimeric procyanidins inhibit phorbol myristate acetate-induced nuclear factor-κB activation in Jurkat T cells, which regulates immune response.[5] They have also been shown to suppress estrogen biosynthesis in vitro and in vivo.[6] More recently, Nomoto et al. demonstrated that grape-seed procyanidins prevent colorectal cancer and increase apoptosis in cancer cells.[7] These findings highlight the diverse biological activities of oligomeric and polymeric procyanidins. In addition, studies on the absorption, metabolism, and excretion of dietary procyanidins in rats have shown that dimeric procyanidins are present in the plasma.[8,9] Fujimura et al. previously reported inhibitory effects of (−)-epigallocatechin gallate on high-affinity IgE receptor (FcεRI) expression and histamine release in human basophilic KU812 cells.[10] Maeda-Yamamoto et al. recently report that O-methylated catechins inhibit protein kinases in mast cells.[11] Kanda et al. reported that apple proanthocyanidins attenuate the release of histamine release from mast cells.[12] However, to our knowledge, relationships between degrees of polymerization of catechin polymers and suppression of exocytosis in mast cells, and mechanisms by which procyanidins inhibit degranulation in mast cells have not been investigated. In addition, proanthocyanidin exerts diverse biological activities such as anti-cancer and anti-allergy activities. No target molecule of procyanidins has been discovered so far. Finding a target molecule of procyanidins is a challenging study. Therefore, we investigated the effects of grape-seed proanthocyanidins (GSPs) on mast-cell signaling and exocytosis and on the actin cytoskeleton in RBL-2H3 cells.

FcεRIs are composed of three subunits: an IgE-binding α subunit, a four-transmembrane signal-amplifying β-subunit, and a disulfide-bonded γ-subunit.[13–15] The

*Keywords*: Grape-seed proanthocyanidin; Mast cell; Degranulation; Membrane ruffling.
* Corresponding author. Tel.: +81 3 3700 9359; fax: +81 3 3707 6950; e-mail: kondo@nihs.go.jp

0968-0896/$ - see front matter © 2005 Elsevier Ltd. All rights reserved.
doi:10.1016/j.bmc.2005.08.051

cross-linking of FcεRIs by antigen (Ag) activates the Src protein tyrosine kinase Lyn, resulting in Syk phosphorylation. The activation of Syk in turn induces the phosphorylation of downstream signaling molecules such as phospholipase C-γ1 (PLC-γ1) and PLC-γ2 via Btk. This leads to the release of two second messengers: inositol 1-, 4-, 5-triphosphate (IP3), and diacylglycerol (DAG). IP3 mobilizes $Ca^{2+}$ from intracellular stores, resulting in an influx of $Ca^{2+}$ through store-operated calcium channels (SOCCs). DAG activates protein kinase C (PKC). Both $Ca^{2+}$ and PKC are required for mast-cell degranulation.[14,16] More recently, Paumet et al. and Martin-Verdeaux et al. demonstrated the role of soluble *N*-ethylmaleimide-sensitive fusion factor-attachment protein receptors in mast cells.[17,18] Cofilin/ADF binds to actin and the dephosphorylation of cofilin at $Ser^3$ activates its actin depolymerizing/severing activities.[19–21] In response to various stimuli such as epidermal growth factor (EGF), cofilin is dephosphorylated and becomes active.[22]

In the present study, we investigated in detail the effects of GSPs on IgE-mediated signaling, exocytosis, and the actin cytoskeleton in RBL-2H3 cells in addition to the relationships between the molecular structures and the activities of monomeric catechin, dimeric, and polymeric procyanidins.

## 2. Results and discussion

### 2.1. Proanthocyanidins (GSP-H) impair mast-cell degranulation

The structure of GSP is shown in Figure 1A. The GSP-H and GSP-L fractions were separated using membrane filters. The mean degree of polymerization numbers (mDP) for GSP, GSP-L, and GSP-H were 7, 3, and 10, corresponding to molecular weights of 2170, 1018, and 3034, respectively. The acid hydrolysis experiment revealed that GSP is mostly comprised of catechin and epicatechin, and not of gallocatechin or epigallocatechin (data not shown). The global minimum-energy conformation of a nanomeric procyanidin built from epicatechin as a model was optimized using the MacroModel (ver. 8.1; MonteCarlo; AMBER) program. The predicted global minimum-energy conformation indicated that the nanomeric procyanidin has a helical structure and an externally oriented B-ring (Fig. 1B). Each 360° turn of the helix requires four catechins. Mass spectrometry analyses revealed that GSP contains non- or galloylated oligomers and polymers (Fig. 1C). Flamini has recently reported mass spectra analysis of grapes and wine.[23] Hayasaka et al. characterized the proanthocyanidins in grape seeds through extensive studies using electrospray ionization (ESI) mass spectrometry.[24] Our results of the mass analysis for GSP are in agreement with these reports. Epicatechin (EC), and the dimeric procyanidins PA-1, PA-2, and PB-2 are shown in Figure 1D.

The effects of GSP on degranulation in rat basophilic leukemia (RBL-2H3) cells were first examined using $DNP_{30}$-HSA as a multivalent antigen (Ag stimulation) and the Ca-ATPase inhibitor thapsigargin (Tg stimulation) to activate the cells. The activity of β-hexosaminidase released from the secretory granules was measured as an index of degranulation. Figure 2A shows that after FcεRI cross-linking, GSP inhibited mast-cell degranulation in a dose-dependent manner. GSP-L and GSP-H were fractionated from GSP to clarify active compounds. Although exocytosis was not inhibited by GSP-L, GSP-H markedly impaired exocytosis by 64% at a concentration of 25 μg/ml (equal to 8.7 μM) and 78% at a concentration of 50 μg/ml (17.4 μM) as shown in Figure 2B. Similar results were obtained in the presence of $Ca^{2+}$ (3 or 5 mM) (data not shown). Based on this, the inhibitory effect of GSP-H on exocytosis was not affected by increasing the extracellular $Ca^{2+}$ concentration. This strongly indicates that GSP-H alters mast-cell function rather than trapping $Ca^{2+}$ ions. Similarly, GSP-H impaired exocytosis after thapsigargin (Tg) stimulation (Fig. 2C), suggesting that GSP-H affects downstream signaling after $Ca^{2+}$ mobilization. Tg can directly induce $[Ca^{2+}]i$. Furthermore, histamine released from the cells stimulated with Ag was measured, and a similar result was obtained as shown in Figure 2D. The inhibition ratio of GSP-H in both assay systems was almost the same. This indicates that GSP-H indeed abolish mast-cell degranulation rather than inhibiting the enzyme activity in the β-hexosaminidase assay.

The inhibitory effect of GSP-H (10 mg/mouse) was confirmed in an in vivo ear-thickness assay 1 h after hapten administration to Balb/c mice, which had been transplanted with IGELa2 hybridoma cells that produce TNP-IgE (Fig. 2E). Whether mechanisms of in vivo and in vitro activities are the same or not remains unknown. There has been no evidence for the absorption of higher degrees of polymerization of procyanidins due to the lack of a detection method for high molecular weight procyanidins.

Epicatechin (EC) and dimeric PA-1, PA-2, and PB-2 did not show any inhibitory effect on degranulation, which suggests a higher degree of polymerization is essential for this activity (Figs. 2F and G). Epigallocatechin gallate also demonstrated a far weaker activity in this assay (data not shown). Epicatechin (EC), and dimeric procyanidins PA-1, PA-2, and PB-1 also had no effect. Obviously a molecular size or length more than that of GSP (heptamer) is needed to inhibit exocytosis in RBL-2H3 cells.

### 2.2. GSP-H does not activate mast cells without stimulation

To investigate the mode of action of GSP-H against RBL-2H3 mast-cell line, GSP-H alone was challenged to the cells. GSP-H, the active fraction of GSP, did not induce degranulation in RBL-2H3 cells without Ag or Tg stimulation (Fig. 3A). By contrast, GSP-H triggered a transient increase in $[Ca^{2+}]i$ as shown in Figure 3B. Degranulation did not occur because a sustained increase in $[Ca^{2+}]i$ is known to be required for

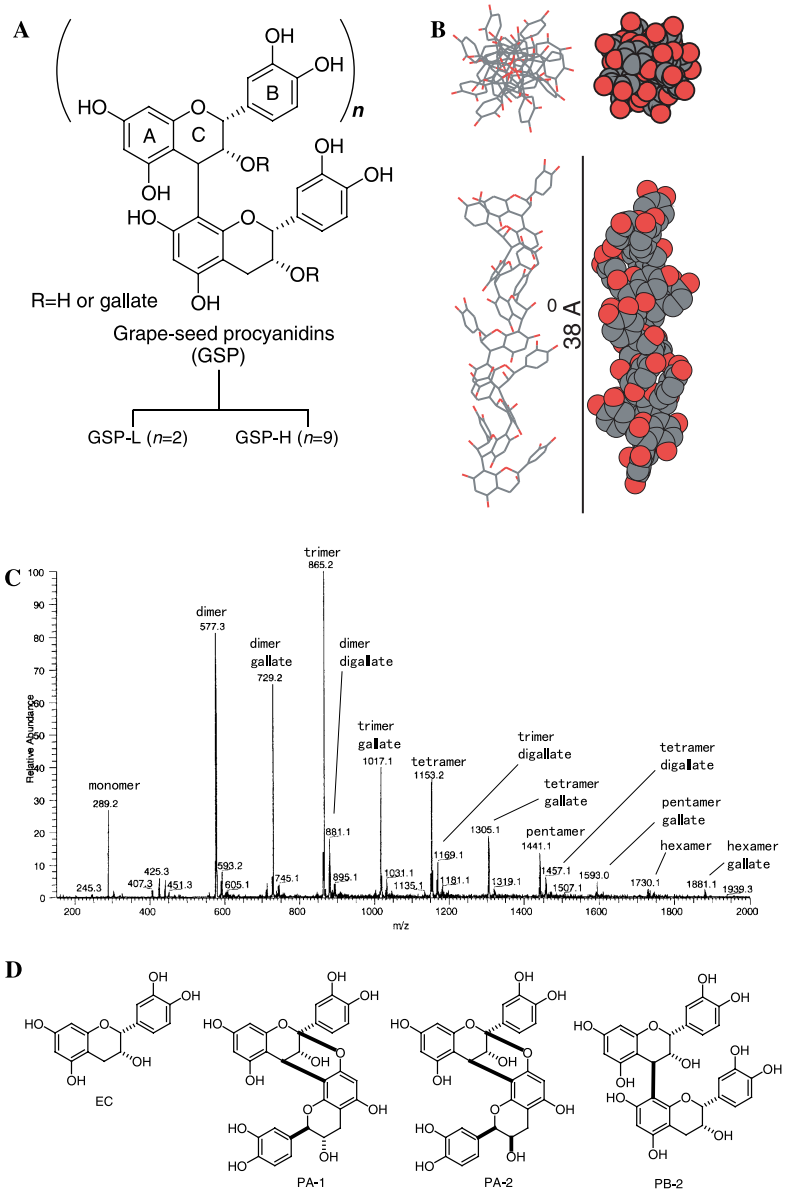


**Figure 1.** Structure of GSP. (A) GSP was extracted from *Vitis vinifera* L. The mean degrees of polymerization for GSP, GSP-L, and GSP-H were estimated as 7, 3, and 10, respectively. (B) The global minimum-energy conformation of a nanomeric procyanidin as a model was calculated using MacroModel (MonteCarlo; AMBER). The nanomeric procyanidin formed a helical structure with its B-ring oriented externally. Red bonds indicate the phenolic hydroxyl groups in the wire-frame image. The gallate moiety is excluded for simplicity. (C) Electrospray mass spectrum of GSP. These proanthocyanidins include galloylated oligomers. (D) Structures of epicatechin (EC) and dimeric procyanidins PA-1, PA-2, and PB-2.

degranulation. However, this $[Ca^{2+}]i$ experiment shows that GSP-H does induce some cell signaling. To examine the IgE-mediated signaling at the moment GSP-H is added to RBL cells, a cell suspension was stimulated with Ag followed by the addition of cold lysis buffer. As shown in Figure 3C, GSP-H did not activate the Syk protein. FcεRI-Syk-PLCγ activation is necessary for $[Ca^{2+}]i$. This transient increase in $[Ca^{2+}]i$ by GSP-H may be independent of FcεRI pathway.

Effect of GSP-H on cell adherence was next examined. In a passage culture of RBL-2H3 cells in the presence of GSP-H, the cells did not attach to the culture plate, resulting in cell death in a dose-dependent manner (Fig. 3D). These results suggest that GSP-H binds to a specific molecule related to adhesion molecules such as an integrin.

To investigate a target molecule of GSP-H, the cell surface proteins were stained with biotin using sulfo-NHS-biotin, and these biotin-labeled proteins were analyzed on immunoblotting by visualizing with streptavidin-alkaline phosphatase. These experiments were repeated three times (exp 1–3). A protein(s) at 150 kDa from the GSP-H treated cells was not stained with biotin (Fig. 3E). The disappearance of this band by GSP-H was dose dependent and the results were highly reproducible. These results strongly suggest that GSP-H binds to a protein at 150 kDa. Tachibana

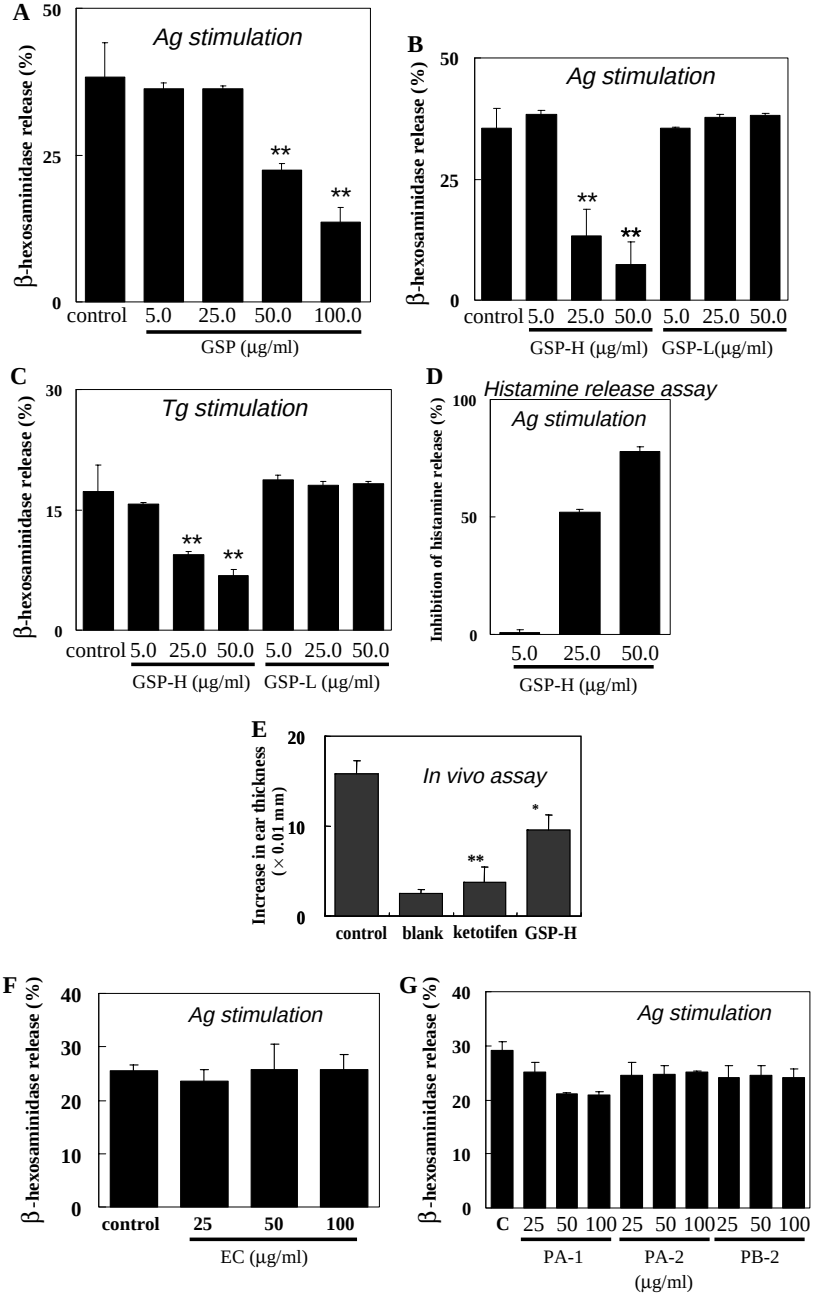


**Figure 2.** Effects of GSP-H and GSP-L on degranulation. (A) The activity of β-hexosaminidase released into the culture media from RBL-2H3 cells treated with GSP was measured when stimulated with $DNP_{30}$-HSA (Ag). (B) The activity of β-hexosaminidase from RBL-2H3 cells treated with GSP-H and GSP-L was measured when stimulated with Ag. (C) β-Hexosaminidase assay was performed when stimulated with Tg instead of Ag. The results are the percentage of the total β-hexosaminidase released in the supernatant after Ag stimulation and are means ± SD of three or four independent experiments. ($n = 3$ or 4; *, $p < 0.05$; **, $p < 0.01$). (D) Histamine release assay. The same experiment as in A and B was done using $DNP_{30}$-HSA. Histamine released from RBL cells was measured to ensure that GSP-H, rather than the enzyme reaction (β-hexosaminidase), inhibited degranulation. The results are given as the inhibition rate (%) ($n = 2$). (E) The ear-swelling response was tested in Balb/c mice (SLC, Japan) in order to determine the effects of GSP-H on the immediate-hypersensitivity reaction. Hybridoma cells (IGELa2) were injected subcutaneously into the back of the neck of each animal. After 10 days, ear thickness was measured. The ear-swelling response was then initiated by picryl-chloride challenge to the ventral side of the neck. Ear thickness was measured 1 h after the challenge. Ketotifen (0.2 mg/ml) was used as a positive control. GSP-H (10 mg/mouse) was orally administered to the mice before antigen stimulation. (F) Effect of epicatechin (EC) on degranulation. (G) Effects of three dimeric procyanidins (PA-1, PA-2, and PB-2) on degranulation.

et al. recently reported that green tea polyphenols can bind to the 67-kDa laminin receptor and inhibit carcinogenesis.[25] Edelson et al. have demonstrated that mast-cell-mediated inflammatory responses require the α2β1 integrin.[26] Therefore, GSP-H is expected to bind to adherent molecules such as integrins and laminin receptors.

The transient increase in $[Ca^{2+}]i$ was not observed when RBL cells were treated with GSP-L, EC, PA-2,

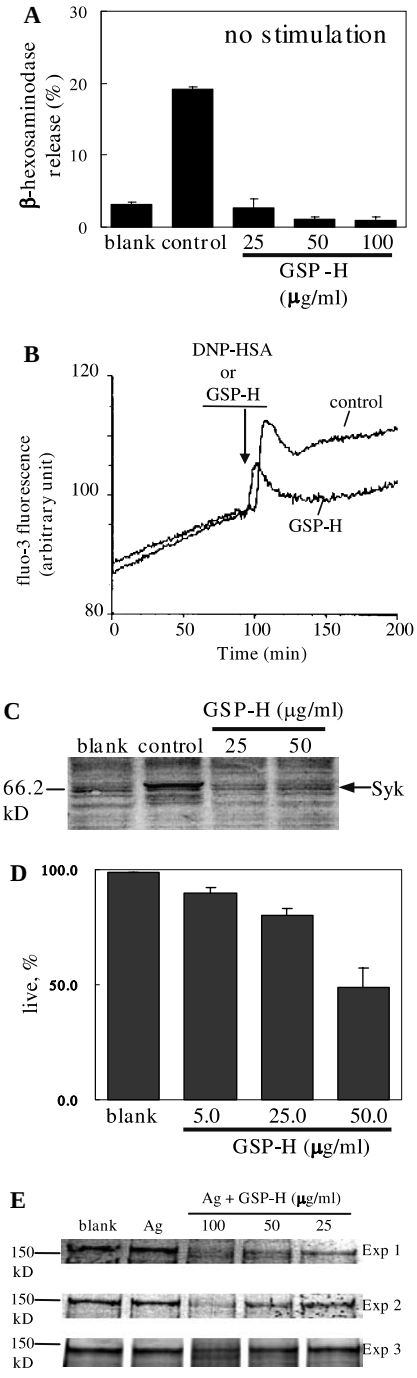


**Figure 3.** Effect of GSP-H on IgE-mediated signaling and cell adherence. (A) β-Hexosaminidase assay was carried out using GSP-H alone. GSP-H does not induce exocytosis without Ag stimulation. (B) GSP-H triggers a transient increase in $[Ca^{2+}]i$. $[Ca^{2+}]i$ was monitored using fluo-3 when Ag or GSP-H was challenged into cells. (C) GSP-H does not induce Syk phosphorylation. Ag or GSP-H was added to a cell suspension and followed immediately by the addition of cold lysis buffer. Phosphorylated proteins were analyzed by immunoblotting using 4G10 mAb. (D) GSP-H inhibits the adherence of RBL-2H3 cells to the culture plate. (E) GSP-H treated cells lack 150 kDa band, which might be the band of a target protein of GSP-H. This result was highly reproducible ($n = 3$, exp 1–3).

and PB-2 (data not shown). Again molecules with a molecular size or length similar to that of GSP-H may be required to induce this response.

### 2.3. FcεRI-induced activation of Syk, PLCγ1, and PLCγ2 is not inhibited by GSP-H

The effects of GSP-H on the FcεRI-mediated tyrosine phosphorylation of several key molecules were investigated to clarify the influence of the proanthocyanidins on mast-cell signaling. After RBL-2H3 cells were sensitized with IgE (0.5 μg/ml) overnight, the cells were treated with GSP-H and then stimulated with Ag for the indicated time. The Syk proteins were phosphorylated, reaching the maximal phosphorylation 5–15 min after FcεRI aggregation. The level of phosphorylation of the Syk proteins in GSP-H treated cells was similar (Fig. 4A).

We also examined the tyrosine phosphorylation of PLCγ1 and PLCγ2, which leads to the formation of IP3 and DAG, resulting in an increase in $[Ca^{2+}]i$ and the activation of PKC. Like Syk, PLCγ2 reached the maximal phosphorylation 5–15 min after Ag stimulation as shown in Figure 4A. The antigen triggered ($DNP_{30}$-HSA, 0.2 μg/ml) PLCγ2 phosphorylation was not affected by GSP-H. No detectable changes in PLCγ1 were observed between the control and GSP-H-treated cells. These findings indicate that GSP-H act on signaling pathway downstream of PLCγ.

### 2.4. Effect of GSP-H on Fak, paxillin, and cofilin

We next investigated the effects of GSP-H on cytoskeletal related proteins. Fak is a non-receptor tyrosine kinase that co-localizes with integrins that bind to extracellular matrix proteins, such as fibronectin and laminin. Hamawy and co-workers reported that FcεRI cross-linking results in the tyrosine phosphorylation of Fak.[27,28] In the present study, the phosphorylation of Fak was examined in the presence and absence of GSP-H. Fak was partly phosphorylated in adherent RBL-2H3 cells and the phosphorylation of Fak increased immediately after FcεRI aggregation. The difference in the level of Fak phosphorylation between the control and GSP-H treated cells increased only after 30-min Ag stimulation. GSP-H inhibited by 40% Fak ($Tyr^{397}$) phosphorylation 30 min after Ag stimulation (Fig. 4B).

We then investigated paxillin, which associates with Fak and links to actin filaments. Paxillin is a protein that associates with Fak at focal adhesion sites and is phosphorylated after FcεRI aggregation.[29] Within 5 min of aggregation of FcεRI, the highest level of phosphorylation was observed, after which the phosphorylation of paxillin gradually decreased to baseline levels (Fig. 4B). When RBL-2H3 cells were treated with GSP-H, the phosphorylation of paxillin was partially impaired from 5 to 30 min after Ag stimulation. The maximum phosphorylation of paxillin in the GSP-H treated cells was two-thirds that of the control (band intensity, 15.4 vs 22.8).

To clarify functions of GSP-H, which shows a protective effect on degranulation, the activation of cofilin was finally investigated. Cofilin regulates actin remodeling, associated with IgE-induced mast-cell degranulation. Cofilin was phosphorylated at the $Ser^{3}$ site in resting cells, and the activation of FcεRI resulted in

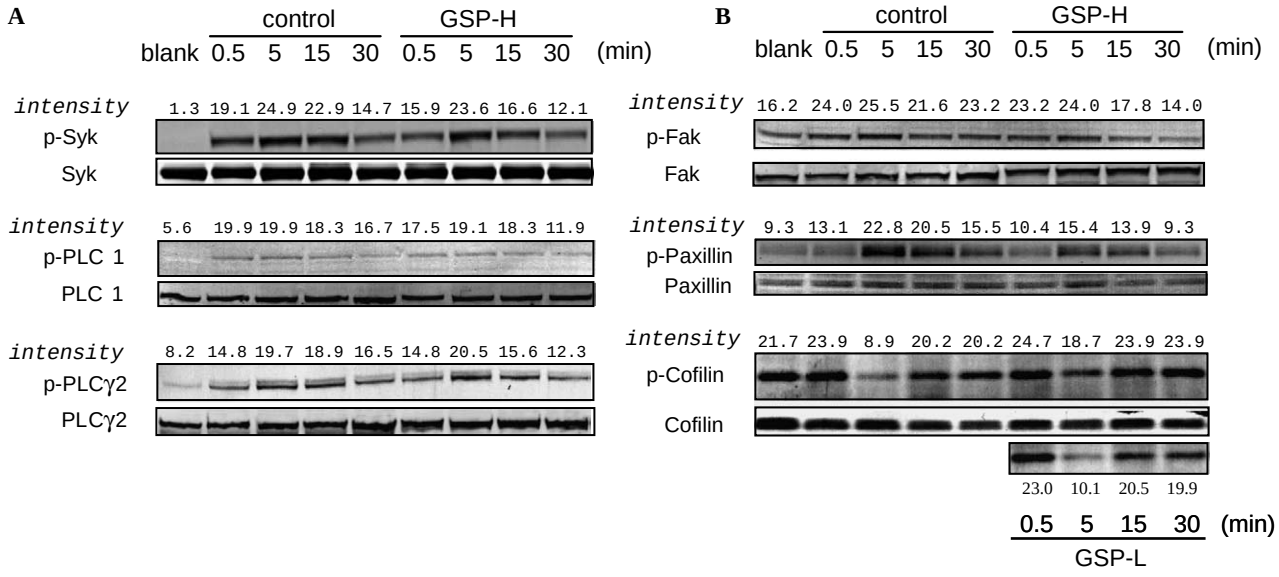


**Figure 4.** Effect of GSP-H on IgE-mediated signaling. (A) FcεRI-induced activation of Syk, PLCγ1, and PLCγ2 is not inhibited by GSP-H. RBL cells were sensitized with IgE (0.5 μg/ml) overnight and then incubated with $DNP_{30}$-HSA (0.2 μg/ml) for the indicated time (0.5, 5, 15, or 30 min) after GSP-H (50 μg/ml) or buffer treatment for 10 min. Cold lysis buffer was added to the cells in a 10-cm culture dish to prepared cell lysates. For Syk phosphorylation, cell lysates were immunoprecipitated with anti-Syk (N-19), followed by protein A–agarose at 4 °C under gentle rotation. The immunoblot was probed with anti-phosphotyrosine Ab (4G10). For the phosphorylation of PLCγ1 and PLCγ2, immunoblots were prepared from whole cell lysates and probed with polyclonal anti-PLCγ1 ($Tyr^{783}$) and PLCγ2 ($Tyr^{1217}$). These results are representative of three experiments, all of which yielded similar results. (B) Effects of GSP-H on Fak, paxillin, and cofilin. The inhibition of FcεRI-induced activation of adherent-related molecules by GSP-H was analyzed by immunoblotting using anti-phosphospecific Fak ($Tyr^{397}$), Paxillin ($Tyr^{118}$), and cofilin ($Ser^{3}$). The same cell lysates were probed with Abs against Fak, paxillin, and cofilin to show an equal amount of proteins in each lane. The experimental procedures were the same as those described in A. These results are representative of three experiments. Fak and paxillin become active when phosphorylated. Cofilin becomes active when dephosphorylated.

the dephosphorylation of cofilin within 5 min, which was active. The phosphorylation of cofilin recovered rapidly. GSP-H markedly inhibited the dephosphorylation of cofilin induced by FcεRI aggregation as shown in Figure 4B (third panel). The band intensity of phosphorylated cofilin after 5 min-Ag stimulation changed from 8.9 in the control cells to 18.7 in the GSP-H treated cells. Dephosphorylated cofilin increases the turnover of actin filaments[20] and activates actin-depolymerizing/severing abilities.[21] Holst et al. demonstrated that the peak rate of Ag-induced granule mediator release was 2.5 min.[30] Our result of cofilin activation is consistent with this report. Active cofilin has actin-depolymerizing/severing activity, and activated cofilin depolymerizes and severes F-actin. In addition, cofilin promotes actin polymerization.[31] New polymerizing nuclei form after being severed by active cofilin. The data presented here specifically suggest that activated cofilin induces actin depolymerization, severing, and polymerization, all of which result in membrane ruffling. Mast-cell degranulation through FcεRI aggregation is associated with membrane ruffling, which is the result of dynamic actin remodeling. Grape-seed procyanidins (GSP-H) may inhibit membrane ruffling by inactivating cofilin, resulting in the suppression of degranulation.

### 2.5. Effects of GSP-H on FcεRI-induced remodeling of the actin cytoskeleton

To investigate the link between mast-cell degranulation, actin remodeling, and the molecular structure of GSP, RBL-2H3 cells were sensitized with IgE (0.5 μg/ml) overnight and treated with either GSP-H or GSP-L before FcεRI aggregation. F-actin of permeabilized RBL-2H3 cells was stained with Texas red-labeled phalloidin to visualize the actin cytoskeleton.

F-actin was located exclusively around the cell periphery in resting cells (Fig. 5, blank). FcεRI aggregation induced membrane ruffling on the dorsal surface within 5 min (Fig. 5, Ag). By contrast, GSP-H treated cells showed different morphological changes on the dorsal surface of the cells after Ag stimulation (Fig. 5, GSP-H + Ag); Although actin remodeling occurred, membrane ruffling was markedly inhibited and large actin plaques formed on the dorsal surfaces of the cells as shown in Figure 5. Similar large actin plaque formation (actin accumulation) in localized areas was observed when cells were stimulated with GSP-H alone (Fig. 5, GSP-H), which indicates that GSP-H itself induces this actin remodeling different from that in the control cells. GSP-L-treated cells (Fig. 5, GSP-L) and cells treated with the dimeric procyanidins (PA-1, PA-2, and PB-2; data not shown) did not show any morphological changes. Given the results in Figure 3, the attachment of GSP-H to the 150 kDa-protein on the surface of RBL-2H3 cells might trigger actin remodeling to form the large plaques observed in these cells.

Apple proanthocyanidins are known not to have a gallate moiety.[32,33] By contrast, grape-seed proanthocyanidins do have gallate moieties. Grape-seed proanthocyanidins

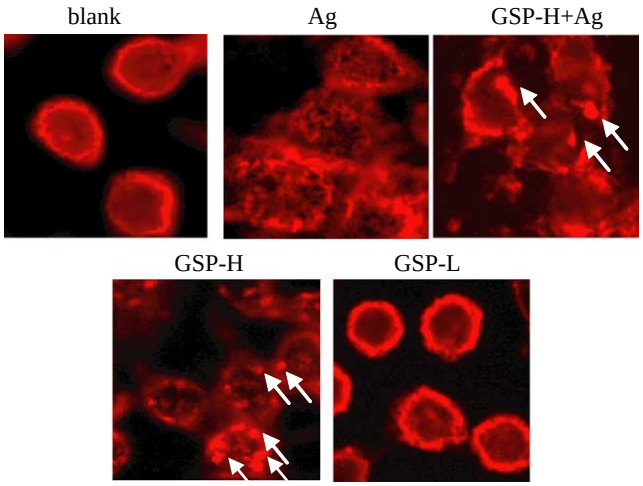


**Figure 5.** The inhibition of IgE-induced membrane ruffling by GSP-H. RBL-2H3 cells were sensitized with IgE (0.5 μg/ml) overnight. After being treated with GSP-H (50 μg/ml) at 37 °C for 10 min, the cells were stimulated with $DNP_{30}$-HSA (0.2 μg/ml) at 37 °C for 5 min. After Ag stimulation, the cells were fixed, permeabilized, and stained with Texas red-labeled phalloidin (F-actin). blank, no stimulation; Ag, $DNP_{30}$-HSA stimulation alone; GSP-H + Ag, $DNP_{30}$-HSA stimulation after GSP-H treatment; GSP-H alone, GSP-H treatment alone. The F-actin was located around the cell periphery in resting cells (blank). FcεRI aggregation induced membrane ruffling and the actin remodeling was observed (Ag). FcεRI-induced membrane ruffling was impaired by GSP-H (GSP-H + Ag). GSP-L resulted in no morphological changes (GSP-L). The arrow indicates F-actin accumulation.

exhibited a similar effect on degranulation as apple proanthocyanidins.[12] This suggests that the gallate moiety might not be involved in the inhibition of exocytosis in mast cells. Furthermore, longer procyanidins such as GSP and GSP-H may be required to induce this activity.

Because there is no evidence for GSP absorption in circular, potential of GSP to mast cells in vivo still remains unclear. However, GSP binds to target molecules and these molecules are most likely on the cell surface. Proanthocyanidins would have a wide variety of three-dimensional conformations because of their complexity. However, only compounds that have a specific conformation would exert a biological activity like that observed here at a lower concentration.

There was no evidence to suggest that GSP-H has cytotoxicity in the in vitro study at any concentration between 12.5 and 100 μM (data not shown). Safety studies have revealed that the GSP we used in the present study has no acute or subchronic oral toxicities or any mutagenicity.[34] Thus, GSP-H could be a potential agent against various diseases including allergy.

## 3. Conclusion

In conclusion, the present study demonstrated novel and important findings. Polymeric proanthocyanidins are predicted to form a helical structure with externally oriented B-rings. Only polymeric GSP-H (ca. 38 Å long) inhibits mast-cell membrane ruffling and degranulation. Monomeric epicatechin and the dimeric procyanidins A-1, A-2, and B-1 have no effect on the ruffling and exocytosis. The present study strongly indicates that GSP-H may bind to a specific molecule (ca. 150 Da) on the cell surface of RBL-2H3 cells.

## 4. Experimental

### 4.1. Characteristics of GSPs

Proanthocyanidins were extracted from grape (*Vitis vinifera* L.) seeds with water and ethanol, and highly purified (GSP, >99% polyphenols, >94% procyanidins, and 5% monomers; brown powder) as described elsewhere.[34] The purity of GSP was determined by the vanillin-HCl method of Broadhurst and Jones.[35] The mean degree of polymerization was estimated as seven (mDP = 7) using thiolysis and the $^{13}C$ NMR (Brucker digital NMR AVANCE 500, 125 MHz) method described by Porter and Newman.[36] The acid hydrolysis of GSP (40 mg) was done using 5% HCl in *n*-BuOH at 100 °C for 2 h (data not shown). Electrospray ionization mass analysis revealed that GSP contained gallate moiety. MALDI-TOF mass analysis showed that the degree of polymerization ranged up to 15 was observed (data not shown). The proanthocyanidins were separated into two fractions, GSP-H ($N = 10$) and GSP-L ($N = 3$), using a membrane filter (Millipore, Billerica, MA). The three procyanidins used in the present study were from the same batch.

### 4.2. Calculation

The structure of a nanomeric procyanidin was optimized by a conformational search in aqueous conditions (MacroModel ver. 8.1, Schrödinger Inc., Jersy City, NJ; MonteCarlo; AMBER force field). The global minimum-energy conformation of the nanomeric procyanidin was calculated from 10,000 initial conformations.

### 4.3. Reagents

Fluo-3 AM was purchased from Dojindo Laboratories (Kumamoto, Japan). Calcium calibration buffer was obtained from Molecular Probes, Inc. (Eugene, OR). Thapsigargin (Tg), human dinitrophenyl human serum albumin ($DNP_{30}$-HSA), anti-DNP monoclonal IgE antibody (clone SPE-7), and protease-inhibitor cocktail were obtained from Sigma (St. Louis, MO). Fetal bovine serum (FBS) was obtained from Invitrogen (Carlsbad, CA). All of the chemicals used in these experiments were of the highest grade. The PIPES buffer consisted of 140 mM NaCl, 5 mM KCl, 0.6 mM $MgCl_2$, 1 mM $CaCl_2$, 5.5 mM glucose, 0.1% (w/v) BSA, and 10 mM PIPES (pH 7.2).

### 4.4. Antibodies

The monoclonal anti-phosphotyrosine (4G10), anti-Fak (clone 4.47), and anti-phospho-Fak ($Tyr^{397}$) used in the immunoblotting analysis were purchased from Upstate Biotechnology (Lake Placid, NY). Anti-Syk (N-19),

anti-PLCγ1 (1269), and anti-PLCγ2 (Q-20) were obtained from Santa Cruz Biotechnology (Santa Cruz, CA). Antibodies for phospho-ERK, phospho-JNK, phospho-p38, phospho-PLCγ1 ($Tyr^{783}$), phospho-PLCγ2 ($Tyr^{1217}$), phospho-paxillin ($Tyr^{118}$), and phospho-cofilin ($Ser^{3}$) were obtained from Cell Signaling (Beverly, MA).

### 4.5. Cell culture

RBL-2H3 cells were maintained in culture in Dulbecco's Modified Eagle's medium supplemented with 10% (v/v) heat-inactivated FBS, 10 mM HEPES buffer, and penicillin–streptomycin–glutamine at 37 °C in a humidified 5% $CO_2$ incubator.

### 4.6. Hexosaminidase assay

The activity of β-hexosaminidase was measured using the method described by Akasaka et al.[37] Briefly, RBL-2H3 cells were preincubated overnight at 37 °C in a 24-well tissue-culture plate ($3 \times 10^5$ cells/well). The supernatant was discarded after sensitization with anti-$DNP_{30}$-IgE for 1 h at 37 °C. The cells were then washed three times with PIPES buffer. Next, 400 μl of the sample solution was added to the cells, which were incubated for 10 min at 37 °C. Finally, 100 μl of $DNP_{30}$-HSA (0.2 μg/ml) was challenged, and the cells were incubated for 40 min at 37 °C. A 200-μl sample of citrate buffer containing *p*-nitrophenyl-2-acetamide-2-deoxy-β-glucopyranoside was added to 50 μl of the supernatant, and the mixture was then incubated at 37 °C for 60 min. The reaction was terminated by the addition of 500 μl of cold glycine (pH 10.0) followed by measurement of absorbance at 405 nm. To quantify the enzyme activity in the cells, 100 μl of 0.2% (v/v) Triton X-100 was added, and the extract was analyzed as described above.

### 4.7. Ear-swelling response in Balb/c mice

The ear-swelling response was tested in Balb/c mice (SLC, Japan) in order to determine the effects of GSP-H on the immediate-hypersensitivity reaction. Briefly, hybridoma cells (IGELa2 from ATCC TIB142) were injected subcutaneously into the back of the neck of each animal. After 10 days, the ear thickness was measured using an upright thickness gauge (Ozaki MFG, Japan). The ear-swelling response was then initiated by picryl-chloride challenge to the ventral side of the neck. Ear thickness was measured 1 h after the addition. Ketotifen (0.2 mg/mouse) was used as a positive control. GSP-H (10 mg/mouse) was orally administered to the mice before antigen stimulation.

### 4.8. Measurement of intracellular calcium concentration

RBL-2H3 cells were suspended at a concentration of $2 \times 10^6$ cells/ml and sensitized with IgE (1 μg/ml) for 30 min at 37 °C. The cells were then loaded with fluo-3 (5 μM) for 15 min at room temperature. After washing three times with PIPES buffer, the cells were resuspended ($1 \times 10^6$ cells/ml) and treated with GSP-H. The intracellular calcium concentration ($[Ca^{2+}]i$) was measured in a cuvette with stirring at 37 °C using a Hitachi F-2500 spectrofluorophotometer. $[Ca^{2+}]i$ was estimated using the method described by Grynkiewicz et al.[38]

### 4.9. Immunoblotting and immunoprecipitation

The IgE-sensitized RBL-2H3 cells cultured on 10-cm dishes were washed with PBS and incubated for 10 min in PIPES buffer in the presence or absence of GSP-H and GSP-L. After $DNP_{30}$-HSA challenge, the RBL cells were incubated for 0.5, 5, 15, or 30 min at 37 °C. The cells were then washed with cold PBS three times, followed by the addition of ice-cold lysis buffer containing 1% Triton-X100, 150 mM NaCl, 1 mM sodium orthovanadate, 100 mM NaF, 1 mM EDTA, and protease-inhibitor cocktail. The cell lysates were either analyzed directly using SDS-PAGE or immunoprecipitated prior to analysis. Isolated proteins were transferred to PVDF membranes (ATTO, Japan), which were visualized using colorimetric-blotting substrates (Bio-Rad, Carlsbad, CA). Immunoprecipitation was carried out on the lysates. The cell lysates were incubated with 3–6 μg of a specific primary antibody at 4 °C overnight under gentle rotation and then with protein A–agarose (Santa Cruz, CA) or protein G–Sepharose (Amersham Biosciences, Piscataway, NJ) at 4 °C for 1 h under gentle rotation. For biotin staining, after treatment with GSP samples for 10 min at room temperature, 0.2 μg/ml DNP-HSA was added to RBL-2H3 cells seeded in a 10 cm-dish and incubated for appropriate time of 30 min. After washing the cells three times with cold DPBS to remove any contaminating proteins, 5 mg of sulfo-NHS-LC-biotin/10 ml DPBS (pH 8.0) was added to the cells in each dish, which were then allowed to stand at room temperature for 30 min. The cells were washed three times with cold DPBS to remove any remaining biotiylation reagent and cell lysates were prepared. The band intensities on immunomembranes were measured using Scion Image software ver. 4.02 (Scion Corp, Frederick, Maryland).

### 4.10. Cell adherent test

A cell suspension ($5 \times 10^5$ cells/ml) was seeded on a 75-ml plate and cultured for 18 h in the absence and presence of GSP-H. Live and dead cells were counted to determine adherent cells.

### 4.11. Immunofluorescence staining of the actin cytoskeleton

RBL cells treated with or without GSP-H were fixed in 3.7% formaldehyde for 10 min and then permeabilized with 0.2% Triton X-100 for 5 min. After blocking with 5% bovine serum albumin (BSA), the cells were stained with Texas red-labeled phalloidin for F-actin staining and Hoechst 33342 for nuclear staining. Finally, the cells were washed with PBS three times and MilliQ water two times, and then mounted onto coverslips using mounting media (ProLong Antifade Kit; Molecular Probes Inc.). The cells were observed using a fluorescence microscope (Olympus IX-71, Japan) equipped

with oil immersion 60× objective lenses, coupled with a cooled CCD camera (Olympus, DP70, Japan).

## Acknowledgments

We thank Dr. M. Kurihara (Division of Organic Chemistry) for calculating the global minimum-energy conformation of the nanomeric procyanidin and Dr. Reiko Teshima (Division of Biochemistry and Immunochemistry) for help with the $Ca^{2+}$ experiments. Procyanidins A-1 and A-2 were kindly donated by Dr. Takashi Tanaka (Nagasaki University). This work was supported in part by the Ministry of Health, Labor and Welfare of Japan.

## References and notes

1. Packer, L.; Rimbach, G.; Virgili, F. *Free Radical. Biol. Med.* **1999**, *27*, 704.
2. Virgili, F.; Kobuchi, H.; Packer, L. *Free Radical Biol. Med.* **1998**, *24*, 1120.
3. Arteel, G. E.; Schroeder, P.; Sies, H. *J. Nutr.* **2000**, *130*, 2100S.
4. Aldini, G.; Carini, M.; Piccoli, A.; Rossoni, G.; Facino, R. M. *Life Sci.* **2003**, *73*, 2883.
5. Mackenzie, G. G.; Carrasquedo, F.; Delfino, J. M.; Keen, C. L.; Fraga, C. G.; Oteiza, P. I. *FASEB J.* **2004**, *18*, 167.
6. Eng, E. T.; Ye, J.; Williams, D.; Phung, S.; Moore, R. E.; Young, M. K.; Gruntmanis, U.; Braunstein, G.; Chen, S. *Cancer Res.* **2003**, *63*, 8516.
7. Nomoto, H.; Iigo, M.; Hamada, H.; Kojima, S.; Tsuda, H. *Nutr. Cancer* **2004**, *49*, 81.
8. Baba, S.; Osakabe, N.; Natsume, M.; Terao, J. *Free Radical Biol. Med.* **2002**, *33*, 142.
9. Gonthier, M. P.; Donovan, J. L.; Texier, O.; Felgines, C.; Remesy, C.; Scalbert, A. *Free Radical Biol. Med.* **2003**, *35*, 837.
10. Fujimura, Y.; Tachibana, H.; Maeda-Yamamoto, M.; Miyase, T.; Sano, M.; Yamada, K. *J. Agric. Food Chem.* **2002**, *50*, 5729.
11. Maeda-Yamamoto, M.; Inagaki, N.; Kitaura, J.; Chikumoto, T.; Kawahara, H.; Kawakami, Y.; Sano, M.; Miyase, T.; Tachibana, H.; Nagai, H.; Kawakami, T. *J. Immunol.* **2004**, *172*, 4486.
12. Kanda, T.; Akiyama, H.; Yanagida, A.; Tanabe, M.; Goda, Y.; Toyoda, M.; Teshima, R.; Saito, Y. *Biosci. Biotechnol. Biochem.* **1998**, *62*, 1284.
13. Ravetch, J. V.; Kinet, J. P. *Annu. Rev. Immunol.* **1991**, *9*, 457.
14. Kinet, J. P. *Annu. Rev. Immunol.* **1999**, *17*, 931.
15. Donnadieu, E.; Jouvin, M. H.; Kinet, J. P. *Immunity* **2000**, *12*, 515.
16. Turner, H.; Kinet, J. P. *Nature* **1999**, *402*, B24.
17. Paumet, F.; Le Mao, J.; Martin, S.; Galli, T.; David, B.; Blank, U.; Roa, M. *J. Immunol.* **2000**, *164*, 5850.
18. Martin-Verdeaux, S.; Pombo, I.; Iannascoli, B.; Roa, M.; Varin-Blank, N.; Rivera, J.; Blank, U. *J. Cell Sci.* **2003**, *116*, 325.
19. Moriyama, K.; Iida, K.; Yahara, I. *Genes Cells* **1996**, *1*, 73.
20. Carlier, M. F.; Laurent, V.; Santolini, J.; Melki, R.; Didry, D.; Xia, G. X.; Hong, Y.; Chua, N. H.; Pantaloni, D. *J. Cell Biol.* **1997**, *136*, 1307.
21. Galkin, V. E.; Orlova, A.; VanLoock, M. S.; Shvetsov, A.; Reisler, E.; Egelman, E. H. *J. Cell Biol.* **2003**, *163*, 1057.
22. Zebda, N.; Bernard, O.; Bailly, M.; Welti, S.; Lawrence, D. S.; Condeelis, J. S. *J. Cell Biol.* **2000**, *151*, 1119.
23. Flamini, R. *Mass Spectrom. Rev.* **2003**, *22*, 218.
24. Hayasaka, Y.; Waters, E. J.; Cheynier, V.; Herderich, M. J.; Vidal, S. *Rapid Commun. Mass Spectrom.* **2003**, *17*, 9.
25. Tachibana, H.; Koga, K.; Fujimura, Y.; Yamada, K. *Nat. Struct. Mol. Biol.* **2004**, *11*, 380.
26. Edelson, B. T.; Li, Z.; Pappan, L. K.; Zutter, M. M. *Blood* **2004**, *103*, 2214.
27. Hamawy, M. M.; Swieter, M.; Mergenhagen, S. E.; Siraganian, R. P. *J. Biol. Chem.* **1997**, *272*, 30498.
28. Vial, D.; Okazaki, H.; Siraganian, R. P. *J. Biol. Chem.* **2000**, *275*, 28269.
29. Hamawy, M. M.; Swaim, W. D.; Minoguchi, K.; de Feijter, A. W.; Mergenhagen, S. E.; Siraganian, R. P. *J. Immunol.* **1994**, *153*, 4655.
30. Holst, J.; Sim, A. T.; Ludowyke, R. I. *Mol. Biol. Cell* **2002**, *13*, 1083.
31. Ghosh, M.; Song, X.; Mouneimne, G.; Sidani, M.; Lawrence, D. S.; Condeelis, J. S. *Science* **2004**, *304*, 743.
32. Ohnishi-Kameyama, M.; Yanagida, A.; Kanda, T.; Nagata, T. *Rapid Commun. Mass Spectrom.* **1997**, *11*, 31.
33. Yanagida, A.; Kanda, T.; Shoji, T.; OhnishiKameyama, M.; Nagata, T. *J. Chromatogr. A* **1999**, *855*, 181.
34. Yamakoshi, J.; Saito, M.; Kataoka, S.; Kikuchi, M. *Food Chem. Toxicol.* **2002**, *40*, 599.
35. Broadhurst, R. B.; Jones, W. T. *J. Sci. Food Agric.* **1978**, *29*, 788.
36. Porter, L. J.; Newman, R. H. *J. Chem. Soc., Perkin Trans. 1* **1982**, *1982*, 1217.
37. Akasaka, R.; Teshima, R.; Kitajima, S.; Momma, J.; Inoue, T.; Kurokawa, Y.; Ikebuchi, H.; Sawada, J. *Biochem. Pharmacol.* **1996**, *51*, 1513.
38. Grynkiewicz, G.; Poenie, M.; Tsien, R. Y. *J. Biol. Chem.* **1985**, *260*, 3440.